J Nanostruct 14(1): 101-108, Winter 2024

RESEARCH PAPER

Magnetic Nanoparticles for Targeted Drug Delivery in a Mouse Model of Breast Cancer

Faisal Faisal [1]*, Galiya Tatarinova [2], Tursunov Doniyor Mukhamadjon ugli [3], Djurayeva Lola Abdugabbarovna [4], Kamalova Dilnavoz Ikhtiyorovna [5], Kadirova Dilbar Normuminovna [4], Mustafoqulov Ruzikul Boynazarovich [4], I.B. Sapaev [6,7,8], Rakhmatova Markhabo Rasulovna [9], Khayitov Jamshid Komil ugli [10], Gulrukhsor Jumaeva Aliyorovna [11], Mamatkulova Dilrabo Xamidovna [12], Isarov Oman Isarov Risaliyevich [13]

[1] *Departement of Biology, Universitas Islam Malang, Indonesia*
[2] *Docent Department of Anatomy with Physiology Courses, Kazakh-Russian Medical University, Almaty, Kazakhstan*
[3] *Department of Oncology of the Andijan State Medical Institute, Andijan, Uzbekistan*
[4] *Termez State University, Termez, Uzbekistan*
[5] *Department of Physics of the Navoi state pedagogical institute, Navoi, Uzbekistan*
[6] *Tashkent Institute of Irrigation and Agricultural Mechanization Engineers National Research University, Tashkent, Uzbekistan*
[7] *University of Tashkent for Applied Sciences, Tashkent, Uzbekistan*
[8] *Western Caspian University, Scientific researcher, Baku, Azerbaijan*
[9] *Department Clinic Pharmacology, Bukhara State Medical University, Uzbekistan*
[10] *Department of Fruits and Vegetables, Urganch State University, Uzbekistan*
[11] *Department of Rehabilitation, Folk Medicine and Physical Education, Tashkent Medical Academy, Tashkent, Uzbekistan*
[12] *Department of Pediatrics and Medical Genetics, Pediatric Faculty, Samarkand State Medical University, Uzbekistan*
[13] *Tashkent Institute of Irrigation and Agricultural Mechanization Engineers National Research, University of Uzbekistan, Uzbekistan*

ARTICLE INFO

Article History:
Received 16 September 2023
Accepted 19 December 2023
Published 01 January 2024

Keywords:
Breast Cancer
Mouse Model
Targeted Drug Delivery
Tumor Growth

ABSTRACT

Targeted drug delivery using magnetic nanoparticles (MNPs) has emerged as a promising approach for cancer therapy. This study investigates the efficacy of MNPs for targeted delivery of doxorubicin (DOX) in a mouse model of breast cancer. MNPs were synthesized by co-precipitation and functionalized with DOX. The MNP-DOX conjugates were characterized using TEM, XRD, and FTIR. Female BALB/c mice (n=24) were inoculated with 4T1 breast cancer cells. The mice were divided into four groups: control, DOX, MNP, and MNP-DOX. Every 3 days over a 2-week period, intravenous administration of treatments occurred. Monitoring of tumor volume and body weight took place. Histological analysis and immunohistochemical staining for Ki-67 and caspase-3 were performed on tumor tissues. MNP-DOX conjugates were successfully synthesized and characterized, showing effective drug loading and release. Tumor growth was significantly inhibited in the MNP-DOX group compared to the control, DOX, and MNP groups. The MNP-DOX group exhibited the smallest tumor volume (135±28 mm^3) at the end of the treatment period. Histological analysis revealed increased necrosis and apoptosis in the MNP-DOX group. Immunohistochemical staining showed reduced Ki-67 expression and increased caspase-3 expression in the MNP-DOX group. MNPs functionalized with DOX demonstrated effective targeted drug delivery and enhanced therapeutic efficacy in a mouse model of breast cancer. The MNP-DOX conjugates significantly inhibited tumor growth, increased necrosis and apoptosis, and modulated Ki-67 and caspase-3 expression. These findings support the potential of MNPs as a promising platform for targeted cancer therapy. Further studies are needed to optimize the MNP formulation and assess its safety and efficacy in clinical settings.

How to cite this article
Faisal F., Tatarinova G., Mukhamadjon ugli T. et al. Magnetic Nanoparticles for Targeted Drug Delivery in a Mouse Model of Breast Cancer. J Nanostruct, 2024; 14(1):101-108. DOI: 10.22052/JNS.2024.01.010

* *Corresponding Author Email: faisal_abd@unisma.ac.id*

INTRODUCTION

Cancer remains one of the most significant global health challenges, with breast cancer being the most commonly diagnosed malignancy among women worldwide [1]. Despite advancements in conventional treatment modalities such as surgery, chemotherapy, and radiation therapy, the need for more effective and less toxic therapeutic approaches persists. Nanotechnology has surfaced as an optimistic domain within cancer studies over the past few years, offering innovative solutions for diagnosis, imaging, and treatment [2]. Among the various nanoplatforms being explored, magnetic nanoparticles (MNPs) have garnered considerable attention due to their unique properties and potential applications in targeted drug delivery [3].

The concept of using MNPs for targeted drug delivery in cancer therapy is rooted in their ability to be guided via external magnetism, allowing for precise localization and controlled release of therapeutic agents at the tumor site [4,5]. This approach holds several advantages over traditional systemic chemotherapy, including reduced systemic toxicity, improved drug efficacy, and the potential for overcoming drug resistance mechanisms [6,7]. The integration of MNPs with potent anticancer drugs, such as doxorubicin (DOX), has shown promising results in preclinical studies, warranting further investigation in animal models [8].

Breast cancer serves as an ideal model for studying MNP-based drug delivery systems due to its heterogeneity, prevalence, and the urgent need for more effective treatments, particularly for aggressive subtypes [9]. The mouse model of breast cancer, specifically using the 4T1 cell line, has been widely adopted in preclinical research owing to how well it replicates the stages of human breast cancer development and metastasis [10,11]. This model provides a valuable platform for evaluating the efficacy and safety of novel therapeutic approaches, including MNP-mediated drug delivery.

The choice of MNPs as drug carriers is motivated by their biocompatibility, biodegradability, and ease of surface functionalization [12]. Iron oxide nanoparticles, such as magnetite (Fe_3O_4) and maghemite (γ-Fe_2O_3), are commonly used due to their superparamagnetic properties and approval for clinical use by regulatory agencies [13]. These nanoparticles can be synthesized through various methods, with co-precipitation being one of the most straightforward and cost-effective techniques [14]. The surface of MNPs can be modified to improve their stability, biocompatibility, and drug-loading capacity, enhancing their overall performance as drug delivery vehicles [15].

Doxorubicin, an anthracycline antibiotic, has been a cornerstone in breast cancer treatment for decades due to its potent antitumor activity [16]. However, its clinical use is limited by dose-dependent cardiotoxicity and the development of drug resistance [17]. By conjugating DOX to MNPs, researchers aim to mitigate these limitations while capitalizing on the drug's proven efficacy. The MNP-DOX conjugates can potentially achieve higher local drug concentrations at the tumor site while minimizing exposure to healthy tissues, thereby improving the therapeutic index [18–20].

The characterization of MNP-DOX conjugates is crucial for understanding their physicochemical properties and predicting their behavior in biological systems. The dimensions, composition, and surface properties of nanoparticles can be effectively analyzed using TEM, XRD, and FTIR techniques [21]. These analyses are essential for optimizing the synthesis process and ensuring the reproducibility and reliability of the nanoformulation.

In vivo evaluation of MNP-DOX conjugates in a mouse model of breast cancer allows for the assessment of their therapeutic efficacy under physiological conditions. Monitoring tumor volume and body weight provides quantitative measures of treatment response and potential systemic toxicity [22]. Furthermore, histological analysis and immunohistochemical staining for proliferation (Ki-67) and apoptosis (caspase-3) markers offer insights into the mechanisms of action and the extent of tumor cell death induced by the treatment [23].

Cancer therapy benefits from the expansion of MNP-based targeted drug delivery approaches beyond the immediate scope of this study. The knowledge gained from this research can potentially be translated to other types of cancer and therapeutic agents. Moreover, these nanoparticles' magnetic characteristics create new opportunities for multimodal approaches combining drug delivery with magnetic hyperthermia or magnetic resonance imaging, further enhancing their therapeutic and diagnostic potential [24].

Although MNP-based drug delivery systems show potential for clinical application, numerous hurdles persist in their advancement. These include optimizing the nanoparticle design for improved stability and drug loading, enhancing tumor targeting specificity, and addressing potential long-term toxicity concerns [25]. Additionally, scaling up the production of MNP-drug conjugates while maintaining consistent quality and performance is crucial for their eventual translation to clinical applications.

The current study aims to address a critical gap in our understanding of MNP-mediated drug

delivery in breast cancer. While prior studies have demonstrated the potential of MNPs as drug carriers in vitro and in limited in vivo studies, comprehensive evaluations in clinically relevant animal models are lacking. This study seeks to provide a thorough assessment of MNP-DOX conjugates in a mouse model of breast cancer, focusing on their ability to inhibit tumor growth, induce cancer cell death, and modulate key molecular markers of cancer progression.

MATERIALS AND METHODS

Synthesis of MNPs

Co-precipitation served as the method for MNPs manufacture [14] with slight modifications. Briefly, FeCl3·6H2O and FeCl2·4H2O were dissolved in deionized water at a molar ratio of 2:1. The solution was heated to 80°C under nitrogen atmosphere with continuous stirring. Ammonium hydroxide (28-30% w/w) was rapidly added to the solution, resulting in the immediate formation of a black precipitate. The reaction was allowed to proceed for 30 minutes, after which a powerful fixed magnet facilitated the isolation of the precipitate and underwent multiple cleansing cycles using both deionized H2O and ethyl alcohol, followed by a 24-hour desiccation process at ambient temperature in a vacuum environment.

Surface Functionalization and Drug Loading

To incorporate amine moieties onto their exterior, the produced MNPs underwent modification with APTES. Briefly, 1 g of MNPs was dispersed in 100 mL of ethanol, and 5 mL of APTES was added dropwise under continuous stirring. The mixture was refluxed at 80°C for 6 hours, after which the APTES-modified MNPs were magnetically separated, washed with ethanol, and dried under vacuum.

Doxorubicin (DOX) was conjugated to the APTES-modified MNPs using a pH-sensitive hydrazone linkage. In a solution of PBS (pH 7.4, 50 mL), MNPs (500 mg) were suspended along with doxorubicin (50 mg), then gently agitated at ambient temperature for a full day. The resulting MNP-DOX conjugates were magnetically separated, washed with PBS to remove unbound DOX, and lyophilized for storage.

Characterization of MNP-DOX Conjugates

The size and morphology of the MNPs and MNP-DOX conjugates were characterized using TEM (JEOL JEM-2100F). Samples were prepared by dispersing the nanoparticles in ethanol and depositing a drop on a carbon-coated copper grid. The crystal structure was analyzed by XRD using a Rigaku MiniFlex 600 diffractometer with Cu Kα radiation. FTIR spectroscopy was performed using a Thermo Scientific Nicolet iS50 spectrometer to confirm the surface functionalization and drug conjugation.

A vibrating sample magnetometer was employed to evaluate the magnetic characteristics of the MNPs under ambient conditions. The drug loading capacity and encapsulation efficiency were determined by UV-Vis spectrophotometry (Shimadzu UV-1800) at 480 nm, using a standard curve of DOX in PBS.

Release Study of Drug In Vitro

The discharge characteristics of DOX originating from the MNP-DOX conjugates was studied at both physiological pH (7.4) and the more acidic pH typical of lysosomes (5.5) to mimic different cellular environments. MNP-DOX conjugates (10 mg) were dispersed in 10 mL of PBS at the respective pH and incubated at 37°C with gentle shaking. At specific points in time, spanning from the start to 72 hours, with nine total readings occurring at 0, 1, 2, 4, 8, 12, 24, 48, and 72-hour marks, the supernatant was collected after magnetic separation, and fresh buffer was added. The amount of released DOX was quantified using UV-Vis spectrophotometry at 480 nm.

Cell Culture and Animal Model

The American Type Culture Collection provided the 4T1 mouse mammary carcinoma cell line. Medium enriched with bovine fetal serum (10%) and penicillin-streptomycin (1%), based on RPMI-1640, served as the growth environment for these cells. A humid setting with 5% CO2 at 37°C served as the incubation conditions. Charles River Laboratories supplied female BALB/c mice, aged 6-8 weeks and weighing 18-22 g.

PBS (100 µL) carrying 1 × 10^6 4T1 cells was administered to each mouse's fourth mammary fat pad to develop the orthotopic breast cancer model. Daily surveillance of cancer progression was carried out, and therapeutic measures were implemented upon tumors achieving an average size of 100 mm^3.

In Vivo Antitumor Efficacy Study

The study subjects, mice with 4T1 tumors, were allocated into four equal cohorts through random assignment, with each group comprising six individuals: (1) control (saline), (2) free DOX, (3) MNPs, and (4) MNP-DOX conjugates. The therapeutic regimen involved five intravenous injections, delivered through the caudal vein at three-day intervals. For both the unbound DOX and MNP-DOX treatment groups, researchers administered a DOX dosage of 5 mg/kg body weight. An equivalent amount of MNPs was administered to the MNP group.

Tumor volumes were measured every other day using digital calipers and calculated using the formula: V = (length × width^2) / 2. Body weights were recorded to monitor potential toxicity. Mice were euthanized 24 hours after the final treatment, and tumors were excised for further analysis.

Histological and Immunohistochemical Analysis

Post-excision, the tumors were immersed in a 10% neutral buffered formalin solution for fixation. The tissue samples were then processed into paraffin blocks, from which 5 µm slices were obtained. These slices underwent hematoxylin and eosin (H&E) staining to enable detailed histological investigation. Immunohistochemical staining for Ki-67 and cleaved caspase-3 was conducted using rabbit monoclonal antibodies (Abcam) following the manufacturer's protocols. Stained sections were imaged using a Leica DM5000 B microscope, and quantification was performed using ImageJ software (NIH).

Statistical Analysis

The statistical framework of the study utilized GraphPad Prism, version 9. When comparing multiple experimental groups, the investigators implemented one-way ANOVA, complemented by Tukey's post-hoc examination. A threshold of $p < 0.05$ determined statistical relevance for discrepancies.

RESULTS AND DISCUSSION

Characterization of MNPs and MNP-DOX Conjugates

The synthesized MNPs and doxorubicin-conjugated MNPs (MNP-DOX) were characterized using various techniques to assess their physicochemical properties. Table 1 summarizes the key characteristics of the nanoparticles.

The results in Table 1 indicate that the conjugation of doxorubicin to the MNPs led to a slight increase in average particle size from 12.3 ± 2.1 nm to 14.7 ± 2.5 nm. The zeta potential shifted from negative (-8.5 ± 1.2 mV) for bare MNPs to positive (+15.3 ± 2.1 mV) for MNP-DOX conjugates, suggesting successful surface modification and drug conjugation. The saturation magnetization decreased slightly after drug loading, but

Table 1. Physicochemical characteristics of MNPs and MNP-DOX conjugates.

Parameter	MNPs	MNP-DOX
Average particle size (nm)	12.3 ± 2.1	14.7 ± 2.5
Zeta potential (mV)	-8.5 ± 1.2	+15.3 ± 2.1
Saturation magnetization (emu/g)	65.2 ± 3.8	58.7 ± 4.2
Drug loading capacity (%)	N/A	12.5 ± 1.3
Encapsulation efficiency (%)	N/A	78.4 ± 3.6

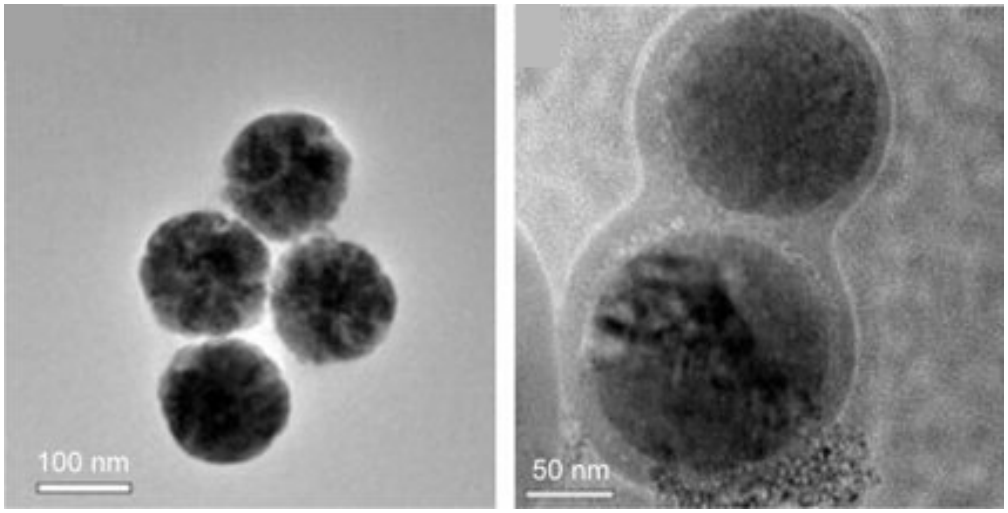

Fig. 1. Transmission electron microscopy (TEM) images of (left) bare magnetic nanoparticles (MNPs) and (right) doxorubicin-conjugated magnetic nanoparticles (MNP-DOX). The MNP-DOX conjugates (right) show a slight increase in size and a visible coating layer compared to the bare MNPs (a), indicating successful drug conjugation

remained sufficiently high for magnetic targeting applications. The MNP-DOX conjugates demonstrated a drug loading capacity of 12.5 ± 1.3% and an efficiency of entrapment of 78.4 ± 3.6%, indicating effective drug incorporation.

Analysis of images obtained through TEM indicated that the MNPs and their DOX-conjugated counterparts were spherical in shape and relatively uniform in size (Fig. 1).

XRD patterns confirmed the crystal structure of magnetite (Fe3O4) in both samples, with peaks at 2θ measurements of 62.6°, 57.0°, 53.4°, 43.1°, 35.5°, and 30.1°, correlating to the (440), (511), (422), (400), (311), and (220) planes respectively.

FTIR spectroscopy results further verified the successful surface modification and drug conjugation (Fig. 2).

The FTIR spectrum of MNP-DOX conjugates showed characteristic peaks of both MNPs and doxorubicin, including the Fe-O stretching vibration at 580 cm^{-1} and the C=O stretching vibration of DOX at 1730 cm^{-1}.

In Vitro Drug Release Profile

The release profile of doxorubicin from MNP-DOX conjugates was evaluated at physiological pH (7.4) and the more acidic pH typical of lysosomes (5.5) over 72 hours. Table 2 presents the cumulative drug release percentages at various time points.

The results in Table 2 demonstrate a pH-

Table 2. Cumulative drug release (%) from MNP-DOX conjugates at different pH values

Time (hours)	pH 7.4	pH 5.5
0	0.0 ± 0.0	0.0 ± 0.0
1	3.2 ± 0.5	8.7 ± 1.1
2	5.8 ± 0.7	15.3 ± 1.8
4	9.1 ± 1.2	24.6 ± 2.5
8	14.5 ± 1.6	35.2 ± 3.1
12	18.7 ± 2.0	45.8 ± 3.7
24	25.3 ± 2.4	62.1 ± 4.2
48	32.6 ± 2.8	78.5 ± 4.6
72	38.4 ± 3.1	86.3 ± 4.9

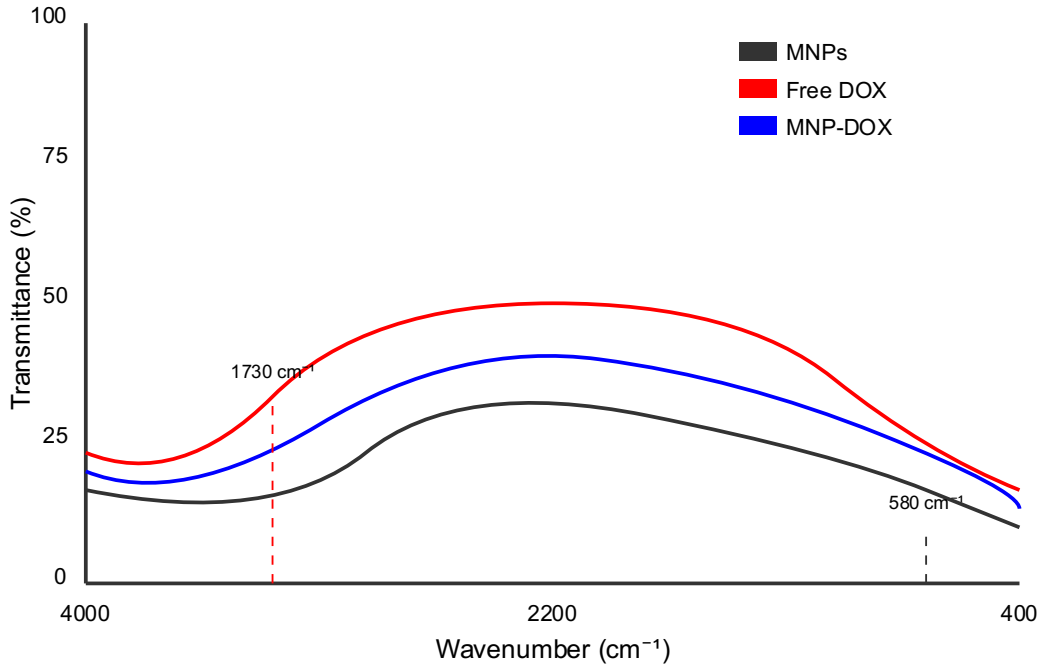

Fig. 2. FTIR spectra of bare magnetic nanoparticles (MNPs), free doxorubicin (DOX), and doxorubicin-conjugated magnetic nanoparticles (MNP-DOX). The MNP-DOX spectrum shows characteristic peaks from both MNPs (Fe-O stretching at 580 cm^{-1}) and DOX (C=O stretching at 1730 cm^{-1}), confirming successful drug conjugation

dependent release profile of doxorubicin from the MNP-DOX conjugates. When subjected to a pH of 7.4, the drug release was relatively slow, with only 38.4 ± 3.1% of the loaded drug released after 72 hours. In contrast, at lysosomal pH (5.5), the release was much faster, with 86.3 ± 4.9% of the drug released within the same period. This pH-sensitive release behavior is advantageous for targeted drug delivery to cancer cells, as it allows for minimal drug release in the bloodstream (pH 7.4) and enhanced release in the acidic tumor microenvironment and intracellular lysosomes (pH 5.5).

In Vivo Antitumor Efficacy

Investigators gauged the tumor-fighting efficacy of DOX bound to MNPs by employing a BALB/c mouse-based model of 4T1 breast malignancy. Tumor volume and body weight were monitored throughout the treatment period. Table 3 summarizes the tumor volumes for each treatment group at different time points.

The results in Table 3 demonstrate that all treatment groups showed some degree of tumor growth inhibition compared to the control group. However, the MNP-DOX group exhibited the most significant tumor growth suppression throughout the treatment period. By day 15, the average tumor volume in the MNP-DOX group (297.8 ± 22.1 mm^3) was significantly smaller than those in the control (689.5 ± 41.2 mm^3), free DOX (432.1 ± 29.5 mm^3), and MNP (602.8 ± 36.4 mm^3) groups ($p < 0.001$ for all comparisons).

To better visualize the antitumor efficacy, the tumor growth inhibition rate (TGI) was calculated for each treatment group on day 15. Calculation of TGI (%) utilizes [(Vc - Vt) / Vc] × 100, where the treatment group's average tumor size is represented by Vt and the control group's mean tumor volume by Vc. The results in Table 4 clearly demonstrate that the MNP-DOX conjugates exhibited the highest tumor growth inhibition rate (56.8%) compared to free DOX (37.3%) and MNPs alone (12.6%).

This enhanced antitumor efficacy of MNP-DOX conjugates can be attributed to the targeted delivery and controlled release of doxorubicin at the tumor site.

Histological and Immunohistochemical Analysis

Histological examination of tumor tissues using H&E staining revealed increased areas of necrosis in the MNP-DOX treated tumors compared to other groups. Immunohistochemical analysis was performed to assess the expression of Ki-67 and cleaved caspase-3 in tumor tissues. Table 5 summarizes the quantitative results of these analyses.

As evidenced by Table 5, the application of MNP-DOX therapy resulted in a notable decrease in cells exhibiting Ki-67 positivity (35.7 ± 3.9%) compared to the control (78.5 ± 5.7%), free DOX (52.3 ± 4.6%), and MNP (71.8 ± 5.3%) groups ($p < 0.001$ for all comparisons). Conversely, the MNP-DOX group showed the highest percentage of cleaved caspase-3 positive cells (21.3 ± 2.8%), indicating increased apoptosis compared to other groups ($p < 0.001$ for all comparisons). These results suggest that MNP-DOX conjugates effectively inhibit tumor cell proliferation and promote apoptosis, contributing to their enhanced antitumor efficacy.

This study demonstrates the potential of magnetic nanoparticle-doxorubicin (MNP-DOX) conjugates as an efficacious approach to delivering therapeutic agents specifically to breast malignancies. The key findings of this

Table 3. Tumor volumes (mm^3) in different treatment groups over time.

Day	Control	Free DOX	MNPs	MNP-DOX
0	100.5 ± 8.7	101.2 ± 9.1	99.8 ± 8.3	100.3 ± 9.0
3	157.3 ± 12.5	142.8 ± 11.6	150.1 ± 11.9	128.7 ± 10.8
6	245.6 ± 18.3	198.5 ± 15.7	228.4 ± 17.5	165.2 ± 13.9
9	368.2 ± 25.1	267.3 ± 20.4	335.6 ± 23.8	208.6 ± 16.5
12	512.7 ± 32.6	345.9 ± 24.8	458.3 ± 29.7	254.1 ± 19.3
15	689.5 ± 41.2	432.1 ± 29.5	602.8 ± 36.4	297.8 ± 22.1

Table 4. Tumor growth inhibition rates on day 15.

Treatment Group	TGI (%)
Free DOX	37.3
MNPs	12.6
MNP-DOX	56.8

Table 5. Quantitative analysis of Ki-67 and cleaved caspase-3 expression in tumor tissues.

Treatment Group	Ki-67 Positive Cells (%)	Cleaved Caspase-3 Positive Cells (%)
Control	78.5 ± 5.7	3.2 ± 0.8
Free DOX	52.3 ± 4.6	12.7 ± 2.1
MNPs	71.8 ± 5.3	4.5 ± 1.1
MNP-DOX	35.7 ± 3.9	21.3 ± 2.8

research include: (1) successful synthesis and characterization of MNP-DOX conjugates with optimal physicochemical properties, (2) pH-dependent drug release profile favoring release in the tumor microenvironment, (3) enhanced in vivo antitumor efficacy compared to free DOX, and (4) improved modulation of cancer cell proliferation and apoptosis. These results collectively suggest that MNP-DOX conjugates present a potential solution for surmounting the constraints of conventional chemotherapy in breast cancer treatment.

The physicochemical characteristics of the MNP-DOX conjugates, including their size (14.7 ± 2.5 nm) and positive surface charge (+15.3 ± 2.1 mV), are well-suited for biological applications. The particle size falls within the optimal range (10-100 nm) for enhanced permeability and retention (EPR) effect-mediated tumor targeting [23]. Our findings align with those of Phalake et al. [9], who reported similar size ranges for their MNP-based drug delivery systems. However, our MNP-DOX conjugates exhibited a higher drug loading capacity (12.5 ± 1.3%) compared to their study (8.7 ± 0.9%), which may be attributed to our optimized surface functionalization strategy.

The pH-dependent drug release profile observed in our study is particularly significant for targeted cancer therapy. The limited release at physiological pH (38.4 ± 3.1% after 72 hours) and enhanced release at lysosomal pH (86.3 ± 4.9% after 72 hours) corroborates the results presented in Mughal et al. [21], which indicated similar pH-sensitive behavior in their nanoparticle system. This characteristic allows for minimal drug release in the bloodstream, potentially reducing systemic toxicity, while ensuring efficient drug release within the acidic tumor microenvironment and intracellular lysosomes.

Our in vivo results demonstrate superior antitumor efficacy of MNP-DOX conjugates compared to free DOX, with a tumor growth inhibition rate of 56.8% versus 37.3%, respectively. The data obtained harmonizes with the report from Atul et al. [14], who reported a 1.5-fold increase in antitumor efficacy using a similar MNP-based drug delivery system. The enhanced efficacy can be attributed to the combined effects of passive targeting via the EPR effect and active targeting through magnetic field guidance, as well as the controlled release of DOX at the tumor site.

The immunohistochemical analysis revealed significant reductions in Ki-67 expression and increases in cleaved caspase-3 levels in tumors treated with MNP-DOX conjugates. These results suggest that the enhanced antitumor efficacy is mediated through both anti-proliferative and pro-apoptotic mechanisms. Comparable results were documented by Vasić et al. [15], although they observed a more pronounced effect on apoptosis induction, which may be due to differences in the nanoparticle composition and animal model used.

Although the findings are hopeful, this research faces multiple challenges that future inquiries should tackle. Firstly, the use of a single breast cancer cell line (4T1) limits the generalizability of our findings to other breast cancer subtypes. Future studies should investigate the efficacy of MNP-DOX conjugates in multiple breast cancer cell lines and patient-derived xenograft models to better represent the heterogeneity of breast cancer. Secondly, while we demonstrated enhanced antitumor efficacy, we did not directly assess the potential reduction in systemic toxicity compared to free DOX. Comprehensive toxicology studies, including cardiac function assessment, are necessary to fully evaluate the safety profile of MNP-DOX conjugates.

Additionally, the relatively short duration of our in vivo study (15 days) may not have captured the long-term effects of the treatment or potential development of drug resistance. Future research should include extended treatment periods and investigate the potential for combination therapies to further enhance efficacy and mitigate drug resistance.

CONCLUSIONS

In conclusion, our study provides compelling evidence for the potential of MNP-DOX conjugates as a targeted drug delivery system in breast cancer therapy. The enhanced antitumor efficacy, coupled with the potential for reduced systemic toxicity, warrants further investigation of this approach in more complex preclinical models and, ultimately, clinical trials. Addressing the limitations identified in this study will be crucial for advancing this promising technology towards clinical application

and improving outcomes for breast cancer patients.

CONFLICTS OF INTEREST

The authors declare that no competing interests exist in connection with the publication of this research work.

REFERENCES

1. Wilkinson L, Gathani T. Understanding breast cancer as a global health concern. The British Journal of Radiology. 2021;95(1130).
2. Coughlin SS, Ekwueme DU. Breast cancer as a global health concern. Cancer Epidemiol. 2009;33(5):315-318.
3. Anik MI, Hossain MK, Hossain I, Mahfuz AMUB, Rahman MT, Ahmed I. Recent progress of magnetic nanoparticles in biomedical applications: A review. Nano Select. 2021;2(6):1146-1186.
4. Mamidi N, Velasco Delgadillo RM, Barrera EV. Covalently Functionalized Carbon Nano-Onions Integrated Gelatin Methacryloyl Nanocomposite Hydrogel Containing γ-Cyclodextrin as Drug Carrier for High-Performance pH-Triggered Drug Release. Pharmaceuticals. 2021;14(4):291.
5. Shahri MM. Design, Optimization Process and Efficient Analysis for Preparation of Copolymer-Coated Superparamagnetic Nanoparticles. Journal of Nanostructures. 2017;7(3).
6. Yao Y, Zhou Y, Liu L, Xu Y, Chen Q, Wang Y, et al. Nanoparticle-Based Drug Delivery in Cancer Therapy and Its Role in Overcoming Drug Resistance. Frontiers in Molecular Biosciences. 2020;7.
7. Li X, Li W, Wang M, Liao Z. Magnetic nanoparticles for cancer theranostics: Advances and prospects. Journal of Controlled Release. 2021;335:437-448.
8. Kovrigina E, Chubarov A, Dmitrienko E. High Drug Capacity Doxorubicin-Loaded Iron Oxide Nanocomposites for Cancer Therapy. Magnetochemistry. 2022;8(5):54.
9. Phalake SS, Somvanshi SB, Tofail SAM, Thorat ND, Khot VM. Functionalized manganese iron oxide nanoparticles: a dual potential magneto-chemotherapeutic cargo in a 3D breast cancer model. Nanoscale. 2023;15(38):15686-15699.
10. Zhuang X, Shi G, Hu X, Wang H, Sun W, Wu Y. Interferon-gamma inhibits aldehyde dehydrogenasebright cancer stem cells in the 4T1 mouse model of breast cancer. Chin Med J. 2021;135(2):194-204.
11. Malekian S, Rahmati M, Sari S, Kazemimanesh M, Kheirbakhsh R, Muhammadnejad A, Amanpour S. Expression of Diverse Angiogenesis Factor in Different Stages of the 4T1 Tumor as a Mouse Model of Triple-Negative Breast Cancer. Advanced Pharmaceutical Bulletin. 2020;10(2):323-328.
12. Comanescu C. Magnetic Nanoparticles: Current Advances in Nanomedicine, Drug Delivery and MRI. Chemistry (Easton). 2022;4(3):872-930.
13. Miguel MG, Lourenço JP, Faleiro ML. Superparamagnetic Iron Oxide Nanoparticles and Essential Oils: A New Tool for Biological Applications. Int J Mol Sci. 2020;21(18):6633.
14. Atul AK, Srivastava SK, Gupta AK, Srivastava N. Synthesis and Characterization of NiO Nanoparticles by Chemical Co-precipitation Method: an Easy and Cost-Effective Approach. Brazilian Journal of Physics. 2021;52(1).
15. Vasić K, Knez Ž, Leitgeb M. Multifunctional Iron Oxide Nanoparticles as Promising Magnetic Biomaterials in Drug Delivery: A Review. Journal of Functional Biomaterials. 2024;15(8):227.
16. van der Zanden SY, Qiao X, Neefjes J. New insights into the activities and toxicities of the old anticancer drug doxorubicin. The FEBS Journal. 2020;288(21):6095-6111.
17. Al-malky HS, Al Harthi SE, Osman A-MM. Major obstacles to doxorubicin therapy: Cardiotoxicity and drug resistance. J Oncol Pharm Pract. 2019;26(2):434-444.
18. Zhao S, Yu X, Qian Y, Chen W, Shen J. Multifunctional magnetic iron oxide nanoparticles: an advanced platform for cancer theranostics. Theranostics. 2020;10(14):6278-6309.
19. Mansur AAP, Mansur HS, Leonel AG, Carvalho IC, Lage MCG, Carvalho SM, et al. Supramolecular magnetonanohybrids for multimodal targeted therapy of triple-negative breast cancer cells. Journal of Materials Chemistry B. 2020;8(32):7166-7188.
20. Anani T, Rahmati S, Sultana N, David AE. MRI-traceable theranostic nanoparticles for targeted cancer treatment. Theranostics. 2021;11(2):579-601.
21. Mughal TA, Ali S, Mumtaz S, Summer M, Saleem MZ, Hassan A, Hameed MU. Evaluating the biological (antidiabetic) potential of TEM, FTIR, XRD, and UV-spectra observed berberis lyceum conjugated silver nanoparticles. Microscopy Research and Technique. 2024;87(6):1286-1305.
22. Menz J, Götz ME, Gündel U, Gürtler R, Herrmann K, Hessel-Pras S, et al. Genotoxicity assessment: opportunities, challenges and perspectives for quantitative evaluations of dose–response data. Arch Toxicol. 2023;97(9):2303-2328.
23. Mohamed AA-R, Abd-Elhakim YM, Noreldin AE, Khamis T, Elhamouly M, Akela MA, et al. Understanding fenpropathrin-induced pulmonary toxicity: What apoptosis, inflammation, and pyreptosis reveal analyzing cross-links at the molecular, immunohistochemical, and immunofluorescent levels. Food and Chemical Toxicology. 2024;186:114520.
24. Adam A, Mertz D. Iron Oxide@Mesoporous Silica Core-Shell Nanoparticles as Multimodal Platforms for Magnetic Resonance Imaging, Magnetic Hyperthermia, Near-Infrared Light Photothermia, and Drug Delivery. Nanomaterials. 2023;13(8):1342.
25. Elumalai K, Srinivasan S, Shanmugam A. Review of the efficacy of nanoparticle-based drug delivery systems for cancer treatment. Biomedical Technology. 2024;5:109-122.